*Bulgarian Chemical Communications, Volume 48, Special Issue E (pp. 373 - 377) 2016*

# Study of the properties of multilayered gradient TiAlSiN nanocomposite coating deposited on 1.2343 steel

S. I. Dishliev[1], G. A. Mishev[2], V. S. Rupetsov[2], L. P. Kolaklieva[3], Ch. O. Pashinski[3,4*], R. A. Minchev[2]

[1]*Department of Machinery for the Food Industry, University of Food Technologies, 26 Maritza Blvd, 4000 Plovdiv, Bulgaria*
[2]*Technical College of Smolyan, Paisii Hilendarski University of Plovdiv, 28 Dicho Petrov St., 4700 Smolyan, Bulgaria*
[3]*Central Laboratory of Applied Physics, Bulgarian Academy of Sciences, 61 St. Petersburg Blvd., 4000 Plovdiv, Bulgaria*
[4]*Department of Mechanics, Technical University - Sofia, Br. Plovdiv, 25 Tsanko Diustabanov St., 4000 Plovdiv, Bulgaria*

The application of hard coatings in the machining industry has rapidly grown recently. Their variety is huge and each of them has advantages and disadvantages. The latter makes them suitable for certain and relatively limited purposes. Although one universal coating which is suitable for almost all kind of machining does not still exist, a coating which is close to this definition is discussed in this work: nc-($Al_{1-x}$Tix)N/a-$Si_3N_4$. Its properties which are important from a practical point of view are studied and an analysis of its wide application is performed here.

**Keywords:** nanocomposites, physical vapour deposition (PVD), superhard coatings, tool wear

## INTRODUCTION

The advantages of the composite materials have long been known and they have found application in the nanotechnologies reasonably. In respect to the hard and superhard coatings, one of the major contemporary trends is exactly the creation of nanocomposite coatings. Nowadays, their use in industry is extensive and their diversity is increased [1-5].

The advanced technology for obtaining of superhard nanocomposite coatings is aimed at a creation of small crystallites in size of several nm which are surrounded by an amorphous tissue with thickness of several tenths of nm. Practically, such one construction ensures a lack of columnar structure and the propagation of dislocations is strongly hampered respectively [6, 7]. This, along with the Hall-Petch effect [2, 7, 8], greatly increases the hardness which is the most important mechanical property of these coatings. Thus it reaches and even exceeds the hardness of the diamond [3, 7, 8, 9]. The practical absence of an internal stress in such coatings ensures good adhesion and permanent mechanical properties for an unlimited time period [8, 9].

As far as the above description is common to the modern nanocomposite coatings, the multilayered gradient coating nc-($Al_{1-x}Ti_x$)N/a-$Si_3N_4$ possess some specific characteristics which make it notably suited for various machining processes. Its excellent adhesion due to a smooth transition from the substrate material to the main layers ensures its strength even in incontinuous processing (e. g. milling, punching). The solid solution of the nc-($Al_{1-x}Ti_x$)N nanocrystallites allows relatively easily to control the formation of their small sizes. Even if other than optimum for a high hardness grain sizes have been prepared, they can change during the work operations and one such high hardness can be reached: this is one unique "self-hardening" effect [3, 8, 9, 10]. The a-$Si_3N_4$ amorphous phase gives a good oxidation resistance [9, 10] and prevents the change of the face centered cubic lattice of the nc-($Al_{1-x}Ti_x$)N into a hexagonal at a high-temperature [9, 10] which would lead to a hardness decrease. The top layer which is enriched with Al, ensures the passivation of the coating surface thus increasing the oxidation resistance significantly [11, 12]. Because of above mentioned facts, this coating can be used at a very high temperature: up to ca. 1200 °C [3, 8, 10, 11], when the Co (when used WC/Co tool) begins to diffuse in

---

[*] To whom all correspondence should be sent:
pashinski@yahoo.com

the layers which worsens the properties of the coating [1, 10]. As a result, this allows a machining without a coolant [1], as the low thermal conductivity of this coating protects the cutting tool [1, 13].

One superhard nc-$(Al_{1-x}Ti_x)N$/a-$Si_3N_4$ gradient nanocomposite coating deposited by Vacuum (Cathodic) Arc Deposition (VAD, CAD) on steel 1.2343 (4X5MΦC, X37CrMoV5-1) is discussed below. Most of the mechanical and tribological parameters are studied. One analysis of its practical implementation is performed.

## EXPERIMENTAL DETAILS

The used samples of 1.2343 steel have a rectangular parallelepiped shape: 25 x 8 x 5 mm (Length x Breadth x Height). This steel is often applied as material for injection molds, punches, conveyor screws, etc. They were hardened to 52 HRC (at the highest temperature attained during the deposition process: 485 °C, this steel does not change its hardness), then polished to Ra = 0,033 μm. Immediately before the deposition, they were mechanically cleaned and then treated in an ultrasonic bath with a solvent of deconex HT 1170.

The completely cleaned samples were loaded into the vacuum chamber of a VAD system π80+ (manufactured by PLATIT, Switzerland), in which a LAteral Rotating Cathodes (LARC® technology) [1, 3, 4, 14] are used. An initial pressure of $1{,}0.10^{-4}$ mbar was reached in the chamber, then the samples were heated in an environment of Ar (a flow rate of 6 sccm) up to 485 °C for 90 min. During this period the pressure was risen, but after its end the Ar and heaters were stopped and the pressure was waited to fall back again to $1{,}0.10^{-4}$ mbar.

Next, one etching in Ar+ glow discharge for 5 min was done at a gradually increase of the flow rate of Ar from 55 to 130 sccm and a bias pulsed voltage to the samples $U_{bias}$ = -760 V, while the temperature in the chamber was stabilized at 470 °C to the end of the whole deposition. Then, a pre-cleaning of the cathodes was carried out for 1 min. This is done by a rotation of their magnetic system and evaporation in the opposite direction from that of the deposition, i. e. to the door where they are mounted - Virtual Shutter® technology [1, 14]. The last ensures the production of unpolluted layers with guaranteed quality. Through the already cleaned cathodes one bombardment of the samples with metal Ti+ ions was done for 4 min at a flow rate of Ar of 20 sccm and a bias voltage $U_{bias}$ which was changed from -850 to -1000 V. During this cleaning, the Ti cathode worked only at arc current of ca. 65 A. With that the actual coating deposition was ready to begin.

The deposition was performed in a pure $N_2$ atmosphere. The process was regulated by pressure, not flow rate, in order to achieve higher accuracy and repeatability. It was carried out at a bias voltage $U_{bias}$ = -110 ÷ -40 V (being varied according to the respective steps of the coating recipe), while the maximum ion current to the samples $I_{bias}$ (two working cathodes of Ti and AlSi) reached 5,0 ÷ 5,5 A. Initially, the deposition begun with the interface TiN layer, passed through gradient layers to the nc-$(Al_{1-x}Ti_x)N$/a-$Si_3N_4$ base layer and finally reached gradiently to the outermost layer which has an increased content of Al for a greater oxidation resistance of the surface. The structure of the obtained coating is partially described in [7]. The total duration of the deposition was about 2 h, a three-axial rotation of samples was used.

After that, the samples were cooled down (the pumps and gas flow were turned off), as when temperature dropped to 380 °C, the chamber was inflated with $N_2$ at a flow rate of 200 sccm for 5 min. Finally, a temperature drop to 200 °C was waited, after which samples were unloaded from the chamber.

The coating thickness which is an important complex characteristic was measured using calo tester developed by CLAP-Plovdiv [15]. A ball with a diameter of 30 mm was used and the formed calotte section (ball crater) was observed and geometrically dimensioned through the optical system of a Compact Platform CPX (MHT/NHT) CSM Instruments in CLAP-Plovdiv.

The nanohardness and elastic modulus of the coating were studied using Compact Platform CPX (MHT/NHT) CSM Instruments in CLAP-Plovdiv. A Berkovich type diamond indenter was used and the measurements were processed by the Oliver and Pharr method.

The adhesion was evaluated using Micro Scratch Tester (MST) module of the last equipment. A Rockwell type diamond indenter rounded on top (radius of 200 μm) was applied. The coefficient of friction was additionally observed during the scratch test.

The wear resistance of the coating was investigated by the pin-on-flat test using a stand which is developed at Technical University - Sofia, Branch Plovdiv [16]. The counter-part was a pin of $Al_2O_3$ rounded on top (radius of 2,45 mm). The width of the tracks was found using a microscope:

contactless PC based measuring system TESA VISIO-300 at 100x magnification (resolution: 0,001 mm).

## RESULTS AND DISCUSSION

An image of a calotte section made by the calotest is displayed in Fig.1. The interface TiN layer and outermost layer with increased content of Al could be outlined. Also, droplets could be seen there which are occurred unavoidably in VAD processes, but here they are relatively a few and do not make the overall behaviour of the deposited coating worse.

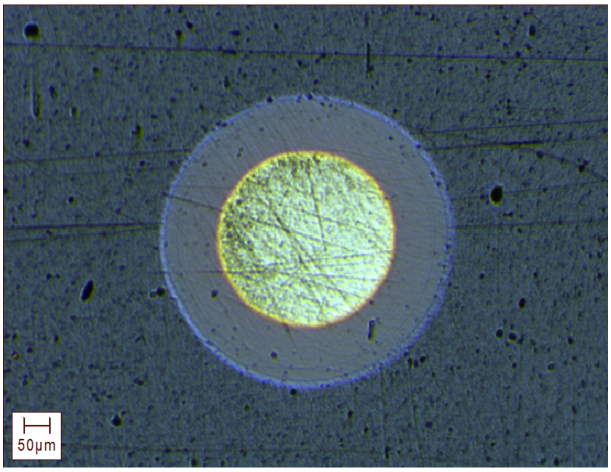

**Fig.1.** Image of the calotte section

Despite this section was designed for the coating thickness measurement, it indirectly demonstrates a good adhesion. In coatings with a poor adhesion, a partial delamination/spallation after such a test could be met frequently.

The coating thickness $h$ was calculated using the equation [15]:

$$h = \frac{D^2 - d^2}{8R} . 10^3 \left[ \mu m \right] \qquad (1)$$

where $D$ – the external section diameter (mm), $d$ – the internal section diameter (mm), $R$ – the grinding ball radius (here: 15 mm). It was evaluated that the coating thickness is 1,960 μm. This is a standard value for deposition on machining tools (2 μm).

Fig.2 shows a load/unload curve caused by the nanoindentation. It is very smooth and this an evidence for no significant damages on the coating during this test [2]. The latter implies good mechanical properties, especially an improved adhesion. The high hardness of the substrate has less influence on the measured coating nanohardness and its smooth surface allows more precise carrying out of such a test.

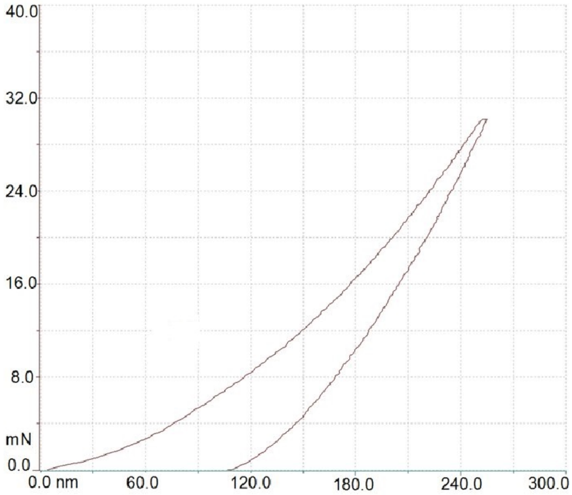

**Fig.2.** Load/unload curve

The following parameters were derived: nanohardness H = 38 GPa; elastic modulus E = 370 GPa; maximum penetration depth $h_m$ = 253 nm (at maximum load of 30 mN). This penetration depth is less than 15 % of the coating thickness (1,960 μm) and implies that the measured nanohardness is related mostly to the coating, i. e. the influence of the substrate is almost completely reduced [9]. This nanohardness is close to the limit for superhard coatings (40 GPa). It could be assumed, that when less penetration (down to 10 %) is used [9], this limit will be exceeded. But, then one has to take the indentation size effect (ISE) in consideration [8, 9]

The results by the scratch test (sliding distance of 3 mm) are shown in Fig.3.

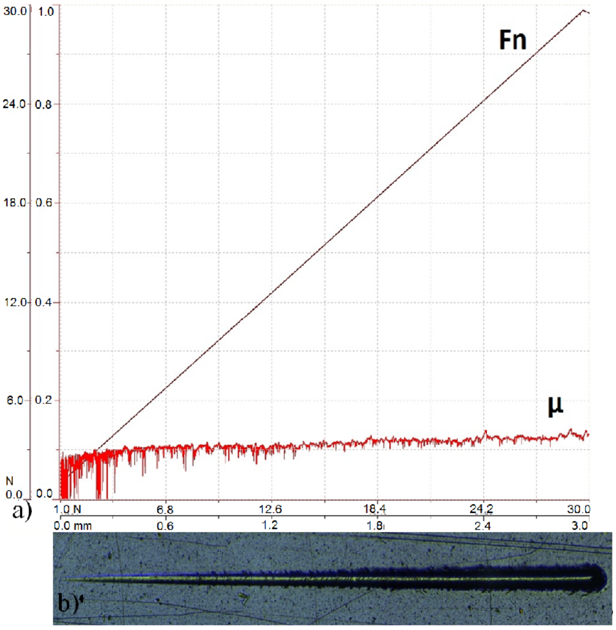

**Fig.3.** Scratch test: a) diagram; b) trace

The load Fn (Fig.3a) which presses the indenter, is changed linearly to its maximum value of 30 N (the maximum load which the used apparatus can create). The coefficient of sliding friction $\mu$ is measured along the trace. Its value is almost constant (especially within the boundaries from concatenation to the first damages), which could be explained by a very little stress in the coating due to the nanocomposite structure. Also, the last predetermines a predominantly smooth trace (Fig.3b). It should be pointed out that the measured low values of the friction coefficient are due to the use of a diamond indenter.

Images of the trace at different load on the indenter are shown in Fig.4. In the beginning, a relatively smooth track without destructions could be seen (Fig.4a and 4b). The first apparent damages in the coating are detected under compressive load of ca. 24 N (Fig.4c). Their insignificance causes a very slight leap in the graph of the coefficient of friction (Fig.3a) - this is the first critical load $L_{C1}$. Since an evident delamination, i. e. substrate exposure, could not be seen in the track, it is acceptable that the second critical load $L_{C2}$ is not reached up to the maximum applied load of 30 N. Also, here could be observed a small amount of droplets which was smashed during the test.

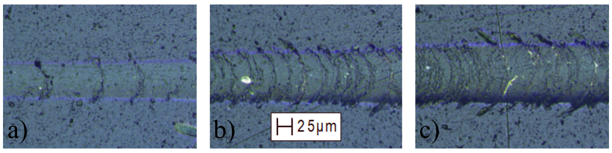

**Fig.4.** View of the trace at different load: a) 9 N; b) 17 N; c) 24 N

A survey of the wear rate was carried out at a room temperature with the following parameters: sliding speed = 6,78 mm/s, stroke of the sample (length of the track) = 11 mm, normal load = 0,65 N. Two test series with different duration t (respectively sliding distance L) were done: t = 30 min (L = 12,21 m) and t = 60 min (L = 24,42 m).

The wear rate $I_w$ was computed by the following equation [17, 18]:

$$I_w = \frac{V}{FL}\left[\frac{mm^3}{Nm}\right] \qquad (2)$$

where $V$ - wear volume ($mm^3$), $F$ - normal load (N), $L$ - sliding distance (m).

After the width of the track was measured initially using a microscope, the wear volume was determined by geometric calculations. For more convenience, one program for the calculation of this volume and wear rate was made using a MS Excel software. Also, using a SolidWorks software, one 3D-model of the track end sections was generated which confirmed the accuracy of these calculations [17].

Table 1 shows the experimental data received by the test for the wear rate assessment. The obtained results prove that under identical conditions, the coated sample is much more wear resistant than the uncoated one. The values for the wear rate are ordinary, but rather to the upper limit for similar coatings. This could be explained by the occurrence of one tribochemical interaction between the counterpart and coating [18]. Also, it could be assumed that the relatively small coating thickness contributes to the higher values of the wear rate (the bottom gradient layers which possess lower wear resistance are affected earlier by the indenter).

**Table 1.** Values of the wear rate under different experimental conditions ($mm^3/Nm$)

| **sample type** | ***t*, min** | ***V*, $mm^3$** | **$I_w$, $mm^3/Nm$** |
|---|---|---|---|
| without coating | 30 | $39,457.10^{-3}$ | $4,971.10^{-3}$ |
| | 60 | $68,848.10^{-3}$ | $4,337.10^{-3}$ |
| after the deposition | 30 | $16,345.10^{-3}$ | $2,059.10^{-3}$ |
| | 60 | $43,615.10^{-3}$ | $2,747.10^{-3}$ |

Additional details about the wear resistance test could be found in [17].

## CONCLUSIONS

The studied nc-$(Al_{1-x}Ti_x)N$/a-$Si_3N_4$ coating demonstrates high hardness, excellent adhesion, low friction coefficient and obviously good wear resistance. Assuredly, these good tribomechanical properties are mainly due to its two-phase nanocomposite structure.

The results of the presented studies are fully proven by the practical application of this coating. According to the data (despite they are unsystematic) received from the partners of CLAP-Plovdiv, it works well when deposited on a variety of cold working machining tools: end mills, drill bits, gear cutters, etc. Also, good results are achieved when it is implemented on injection molds, punches, bed dies, etc., but in such cases, depending on the particular situation, it is successfully competed by other coatings: TiCN, TiN/CrN-ml, nc-$(Al_{1-x}Cr_x)N$/a-$Si_3N_4$, etc. Among its other properties, this coating allows multiple overlapping (re-coating) after a re-sharpening of the tool without removal of the old coating (stripping) [7].

The nanocomposite superhard coatings are one relatively new phenomenon which has become widespread quickly. Described here coating nc-$(Al_{1-x}Ti_x)N$/a-$Si_3N_4$ is already proven in practice and now being worked mostly on its improvement [4, 14]. The presented analysis shows that in the near future this and similar coatings going to become even more relevant to the machining industry.

## REFERENCES

1 S. Veprek, M.J.G. Veprek-Heijman, *Surface & Coatings Technology*, 202(21), 5063 (2008).

2 S. Zhang, D. Sun, Y. Fu, H. Du, *Surface and Coatings Technology*, 167(2-3), 113 (2003).

3 E.N. Reshetnyak, V.E. Strel'nitskij, *Problems of Atomic Science and Technology* (in Russian), 2, 119 (2008).

4 T. Cselle, O. Coddet, C. Galamand, P. Holubar, M. Jilek, J. Jilek, A. Luemkemann, M. Morstein, *Journal of Machine Manufacturing*, XLIX(E1), 19 (2009).

5 B. Sovilj, J. Javorova, P. Kovac, I. Sovilj-Nikic, Proceedings of the XXVI International Science Conference in honour of 65 anniversary of MTF of TU-Sofia and 100 birth anniversary of Acad. Angel Balevski, Sozopol, Bulgaria, 515 (2010).

6 K. Su, D.M. Liu, T.M. Shao, *Science China Technological Sciences*, 58(10), 1682 (2015).

7 Ch. Pashinski, R. Kakanakov, L. Kolaklieva, *Fundamental Sciences and Applications*, 19(2), 71 (2013).

8 A.D. Pogrebnjak, A.P. Shpak, N.A. Azarenkov, V.M. Beresnev, *Uspekhi Fizicheskikh Nauk* (in Russian), 179(1), 35 (2009).

9 S. Veprek, M.G.J. Veprek-Heijman, P. Karvankova, J. Prochazka, *Thin Solid Films*, 476(1), 1 (2005).

10 S. Veprek, H.-D. Männling, M. Jilek, P. Holubar, *Materials Science and Engineering A*, 366(1), 202 (2004).

11 Y. Tanaka, N. Ichimiya, Y. Onishi, Y. Yamada, *Surface and Coatings Technology*, 146–147, 215 (2001).

12 Y.Y. Chang, S.M. Yang, *Thin Solid Films*, 518(21), S34 (2010)

13 L. Chen, S.Q. Wang, Y. Du, S.Z. Zhou, T. Gang, J.C. Fen, K.K. Chang, Y.W. Li, X. Xiong, *Surface & Coatings Technology*, 205(2), 582 (2010).

14 PLATIT AG Compendium 2012, 49th Edition, available through http://www.platit.com (accessed October 24, 2012).

15 V. Kopanov, L. Kolaklieva, *Fundamental Sciences and Applications* (in Bulgarian), 21(2), 37 (2015).

16 S. Dishliev, *Fundamental Sciences and Applications* (in Bulgarian), 14(2), 153 (2009).

17 G. Mishev, S. Dishliev, V. Rupetsov, *Tribological Journal BULTRIB* (in Bulgarian), IV, 147 (2014).

18 D. Philippon, V. Godinho, P.M. Nagy, M.P. Delplancke-Ogletree, A. Fernández, *Wear*, 270(7-8), 541 (2011).